Thermodynamic and Raman Spectroscopic Studies on Difluoromethane (HFC-32) + Water Binary System

Shunsuke Hashimoto,* Hiroshi Miyauchi, Yoshiro Inoue, and Kazunari Ohgaki

Division of Chemical Engineering, Department of Materials Engineering Science, Graduate School of Engineering Science, Osaka University, 1-3 Machikaneyama, Toyonaka, Osaka, 560-8531 Japan

The three-phase equilibrium (pressure−temperature) relation of the difluoromethane + water binary system containing gas hydrates was measured in the pressure range from (0.20 to about 11.0) MPa and temperature range from (275.15 to 300.15) K. On the basis of each three-phase equilibrium curve, the quadruple point which consists of gaseous and liquid difluoromethane, water, and hydrate was determined as 1.45 MPa and 293.16 K. The in situ Raman spectroscopy under the three-phase (gas, water, and hydrate) equilibrium conditions showed that the crystal structure of difluoromethane gas hydrate was structure-I, where both small and large cages were occupied by the difluoromethane molecule. The overall hydration enthalpy of simple structure-I difluoromethane gas hydrate under the three-phase equilibrium conditions was evaluated by means of the Clapeyron equation.

Introduction

Gas hydrates are clathrate inclusion compounds, and they consist of host water molecules and appropriate relatively small guest molecules. Water molecules are hydrogen-bonded and consequently construct hydrate lattices with cavities, in which guest molecules are encaged. Generally, the van der Waals interaction (attractive and repulsive forces) operates on the guest and water molecules. That is, the guest molecules encaged in the clathrate hydrate do not participate in forming hydrate lattices.[1] Three types of hydrate cages are well-known, pentagonal dodecahedron (5^{12}, S-cage), tetrakaidecahedron ($5^{12}6^2$, M-cage), and hexakaidecahedron ($5^{12}6^4$, L-cage). Several types of hydrate unit-cells can be formed from a few types of hydrate cages depending on the size and physical properties of the guest species. For example, the structure-I (s-I) hydrate lattice is composed of two S-cages and six M-cages, and the structure-II (s-II) hydrate lattice is sixteen S-cages and eight L-cages. Recently, the slurries containing gas hydrates have been considered as a potential cooling medium (heat-storage material) for the refrigerators and air conditioners because of their large enthalpy of hydration and dissociation temperature.

Some hydrofluorocarbons (HFCs) have received much attention as a refrigerant of radiators (particularly, large-scale ones for the institutional use) because of their thermal and chemical characteristics that are favorable for a refrigerant material. Although some HFCs have a relatively high global warming potential, promised on "zero-emission" concepts, they have the bright prospect of application as a refrigerant material. In addition, it is possible to reduce the quantity of the cooling medium by use of the phase-change heat of gas hydrates prepared from HFCs. Some investigators[2−6] have studied the equilibrium (pressure−temperature) relations of various chlorofluorocarbons (CFCs), chlorohydrofluorocarbons (CHFCs), or HFC + water (or + second component) systems containing gas hydrates and estimated their formation enthalpy. In addition, Uchida et al.[7] reported the cage occupancy of some HFC hydrates and their hydrate structure by means of Raman spectroscopy at 243 K and atmospheric pressure, which was obtained under nonequilibrium conditions. These results are quite important; however, it is essential to investigate much more fundamental information (such as more accurate phase equilibria and hydration enthalpy values, and the cage occupancy of guests in hydrates and the hydrate structure under the three-phase equilibrium conditions) of HFC hydrate systems for the application of hydrate slurry to refrigerant systems.

In the present study, the thermodynamic stability of difluoromethane (CH_2F_2, hereafter HFC-32) + water binary system containing gas hydrates was investigated by accurate phase-equilibrium measurement. The quadruple point that consists of hydrate, water, gaseous, and liquid HFC-32 was accurately evaluated from these phase-equilibrium data. In addition, the cage occupancy and unit-cell structure of HFC-32 hydrate under the three-phase (gas, water, and hydrate) equilibrium conditions were investigated by in situ Raman microspectroscopic analysis. Finally, the hydration enthalpy of HFC-32 hydrate was estimated from the three-phase equilibrium curve and briefly discussed.

Experimental Methods

Experimental Apparatus. The schematic illustration of the experimental apparatus for phase equilibrium measurements is shown in Figure 1. The experimental apparatus for phase-equilibrium measurements consisted of the following parts: a high-pressure glass cell (model: Taiatsu Techno HPG), a pressure gauge (model: Valcom VPRT), and a temperature control unit (model: Taitec CL-80R). The inner volume and maximum working pressure were 10 cm^3 and 5 MPa, respectively.

The experimental apparatus for Raman spectroscopic analysis consisted of the following parts: a high-pressure optical cell (manufactured by Nezu Industries Co., Ltd.), a pressure gauge (model: Valcom VPRT), and a temperature control unit (model: Tokyo Rikakikai EYELA NCB-3100). The inner volume and maximum working pressure were 0.2 cm^3 and 400 MPa, respectively. The high-pressure optical cell had a pair of sapphire

* Corresponding author. Telephone and fax: +81-6-6850-6277. E-mail: shunsuke@cheng.es.osaka-u.ac.jp.

10.1021/je9009859
Published on Web 05/12/2010

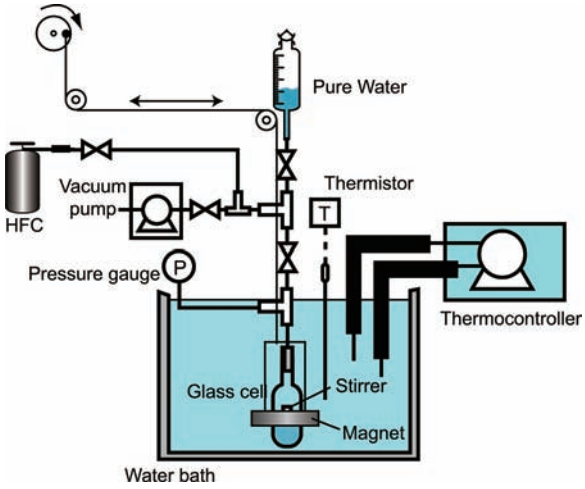

Figure 1. Schematic illustration of the experimental apparatus for phase-equilibrium measurements.

(Ti free) windows on both the upper and the lower sides. This high-pressure optical cell was the same as previous one.[8] The temperature-controlled water was circulated constantly in the exterior jacket of the high-pressure optical cell. To agitate the contents in the cell, a ruby ball was placed inside it. This enclosed ruby ball was rolled around through the contents by a vibrator applied to the outside of the cell.

The system temperature was measured within an uncertainty of 0.02 K using a thermistor probe (model: Takara D-632). The probe was calibrated with a Pt resistance thermometer (25 Ω) defined by ITS-90. The system pressure was measured by the pressure gauge calibrated by the RUSKA quartz Bourdon tube gauge (model: direct reading pressure gauge, series 6000) with an estimated maximum uncertainty of less than 0.01 MPa.

Experimental Procedure. First of all, the dissolved air in water was sufficiently degassed and replaced with the HFC-32 gas by a bubbling method. After that, the pretreated water was introduced into the high-pressure glass cell, which was evacuated by the use of vacuum pump in advance. The contents were pressurized up to a desired pressure by supplying HFC-32 gas, which was expected to be sufficiently higher than the equilibrium pressure. Then, the interior temperature of the high-pressure cell was controlled by immersing the cell in a thermostatted water bath. The contents were subcooled and agitated to generate the gas hydrate. A magnetic stirrer was manipulated in a vertical direction by use of a permanent magnetic ring from outside (up and down) to agitate the contents. The phase behavior was observed directly under the transmitted light. After the formation of gas hydrate, the system pressure dropped and reached a plateau, which was regarded as the three-phase equilibrium state of hydrate (H), gas (G), and water (L_1). The gas hydrate was annealed by giving perturbations in temperature to avoid metastability. The pressure and temperature was determined as the three-phase equilibrium pressure and temperature, respectively. Since then, the contents were heated, and consequently gas hydrates partially dissociated. The system pressure rose and reached another equilibrium value. By repeating same procedures, the HL_1G equilibrium curve could be obtained (when the amount of gas hydrates was decreased, the contents were pressurized up to a desired pressure). In the present study, not only the three-phase equilibrium curve of HL_1G but also the other three-phase equilibrium curves consisting of HL_2G and L_1L_2G (the letter, L_2 stands for the liquid HFC phase) were obtained by similar procedures, except that, in the measurements of HL_2G curve, we paid attention to minimize the amount of water (all of water was transformed into gas hydrates). The measurements of the L_1L_2G curve were started from the vicinity of the quadruple point, which was roughly estimated from the point at the intersection of the HL_1G curve with the saturated vapor-pressure curve.

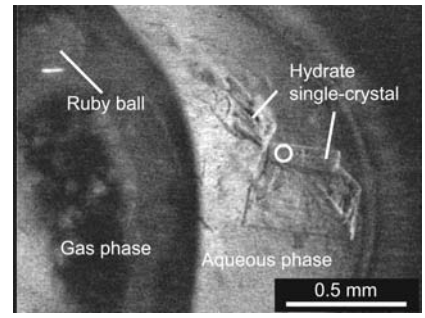

Figure 2. A photo of single crystals for the HFC-32 hydrate obtained at 281.80 K and 0.40 MPa. The circle stands for the analyzing point for the Raman spectroscopic analysis.

The three-phase equilibrium curve of HL_1L_2 was measured by the use of a high-pressure optical cell, which was served to the Raman spectroscopic measurements. A known amount of gaseous HFC-32 was introduced into the evacuated high-pressure optical cell, and then the distilled water was charged to the cell by use of the high-pressure pump up to a desired pressure. At this moment, the interface was between the water and the liquid HFC-32 in the cell. After the pressurization, the two-phase coexistence state of HFC-32 hydrate + water appeared immediately under the experimental conditions. Thereafter, the system temperature was increased gradually. The gas hydrate started to dissociate with a rise in temperature, resulting in the appearance of liquid HFC-32 particles. The gas hydrate was annealed by giving perturbations in temperature to avoid the hysteresis effect. The contents were agitated intermittently for at least half a day to establish the three-phase equilibrium state. After the sufficient amounts of time, the pressure and temperature were determined as the three-phase equilibrium pressure and temperature, respectively.

For in situ Raman spectroscopy, first of all, the pure water degassed in advance was introduced into the evacuated high-pressure optical cell. The contents were pressurized up to a desired pressure by supplying HFC-32 and then cooled and agitated with an enclosed ruby ball to prepare the gas hydrate. After the formation of gas hydrate, the system temperature was increased gradually to leave a few seed crystals. Then, the system temperature was decreased little by little to a desirable temperature to grow the single crystal of gas hydrate. It took more than one day to establish a three-phase (HL_1G) equilibrium condition with the existence of hydrate single-crystal. We were careful to prepare as few single crystals as possible. A single crystal of HFC-32 hydrate was shown in Figure 2, and this single crystal was analyzed by in situ Raman spectroscopy using a laser Raman microprobe spectrophotometer with a multichannel charge-coupled device (CCD) detector. The argon ion laser beam (wavelength: 514.5 nm, laser-spot diameter: 2 μm) from the object lens irradiated the sample through the upper sapphire window. The backscatter of the opposite direction was taken in with the same lens. The spectral resolution was about 0.7 cm^{-1}.

In the present study, to confirm the experimental reproducibility (that is, the fact that the equilibrium data was not affected by a hysteresis phenomenon), we repeated the same equilibrium measurements using fresh water.

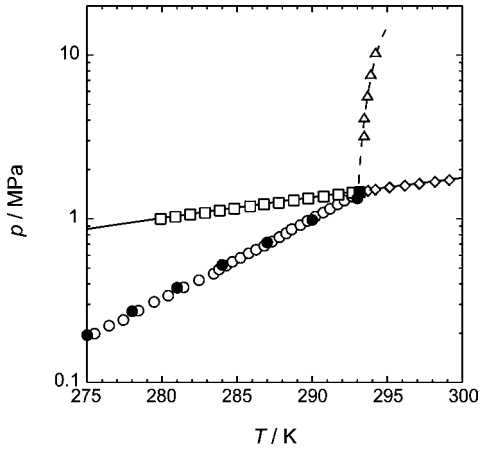

Figure 3. Three-phase equilibrium relation (temperature T−pressure p projection) for the HFC-32 (2) + water (1) binary system. ●, HL_1G (Akiya et al., 1999); ○, HL_1G (present study); □, HL_2G (present study); △, HL_1L_2 (present study); ◇, L_1L_2G (present study); ■, quadruple point (Q_2, present study). −, the saturated vapor pressure of HFC-32.

Materials. HFC-32 (mole fraction purity: 0.9999) was purchased from the Daikin Industries, Ltd. The critical temperature and pressure of HFC-32 were 351.26 K and 5.78 MPa, respectively.[9,10] Distilled water was obtained from the Wako Pure Chemical Industries, Ltd. All of the materials were used without further purification.

Results and Discussion

Figure 3 shows the phase-equilibrium relation for the HFC-32 + water binary system. Table 1 summarizes the three-phase equilibrium (pressure (p)−temperature (T)) relation of HL_1G, HL_2G, HL_1L_2, and L_1L_2G. As shown in Figure 3, the HL_1G curve agrees with the literature value.[3] The HL_2G and L_1L_2G curves lie just below the saturated vapor-pressure curve of the HFC-32 fluid. The quadruple point, Q_2 (293.16 K and 1.45 MPa) for the HFC-32 + water binary system can be estimated accurately as the intersection of four three-phase equilibrium curves (HL_1G, HL_2G, and L_1L_2G).

Figure 4 represents the Raman spectra of the HFC-32 + water binary system in the hydrate phase, which are obtained under the three-phase (HL_1G) equilibrium condition. In some previous studies,[11−14] Raman-active vibration frequencies of HFC-32 gas were investigated experimentally and theoretically, and they reported nine vibration modes derived from HFC-32 as follows: CH_2 symmetric stretching (ν_1), CH_2 scissors (ν_2), CF_2 symmetric stretching (ν_3), CF_2 scissors (ν_4), CH_2 twisting (ν_5), CH_2 asymmetric stretching (ν_6), CH_2 rocking (ν_7), CH_2 wagging (ν_8), and CF_2 asymmetric stretching (ν_9). In the present study, we succeeded in observing five vibration modes (ν_1, ν_3, ν_4, ν_6, and ν_9) of HFC-32. Figure 4a shows the Raman spectra corresponding to intramolecular C−H symmetric (ν_1) and asymmetric (ν_6) stretching vibrations in the hydrate phase. The doublet peak of C−H symmetric stretching vibration is detected at (3017 and 3025) cm^{-1}, and that of C−H asymmetric stretching vibration is obtained at (2947 and 2958) cm^{-1} in the hydrate phase. In each doublet peak, the peak at the higher Raman shift corresponds to the HFC-32 in the small cage, while the peak at the lower Raman shift does in the large cage. The ratio of large to small cages on the peak area or intensity of HFC-32 is about 3. This indicates that the crystal structure of simple HFC-32 hydrate is s-I type, which contains two S-cages and six M-cages. Although the peak obtained at around 2830 cm^{-1} is not shown in Figure 4a, this peak may correspond to the harmonic overtone of CH_2 wagging mode ($2\nu_8$).[11] The present results about C−H vibration agree well with those of reference data.[7] Figure 4b shows the Raman spectra corresponding to intramolecular F−C−F scissors vibration (ν_4) in the hydrate phase. As in the case with the peak of C−H vibron, the doublet peak of F−C−F scissors is detected at (528 and 533) cm^{-1} in the hydrate phase. The intensity ratio of these two peaks also indicates that HFC-32 can be occupied in both S- and M-cages of s-I hydrate. Figure 4c shows the Raman spectra corresponding to intramolecular C−F symmetric (ν_3) and asymmetric (ν_9) stretching vibrations in the hydrate phase. Unlike the peak of C−H vibron and F−C−F scissors, the single Raman peaks corresponding to C−F symmetric and asymmetric stretching vibrations are obtained at (1098 and 1087) cm^{-1} in the hydrate phase, respectively. As in the case with the simple HFC-32 hydrate, the single peak is obtained in the simple N_2 hydrate system[15] (N−N symmetric stretching vibration mode) and the simple CO_2 hydrate system[8] (C−O symmetric stretching vibration mode, the doublet peak derived from the only fermi-resonance effect) despite the occupation of both small and large cages in these hydrates. The reason why only a single peak is obtained despite the occupation of guest species in both small and large cages is still unclear. Parts d and e of Figure 4 represent the Raman spectra derived from the O−H stretching vibration and intermolecular O−O stretching vibration of the host water molecule for the simple HFC-32 hydrate, respectively. Compared to the peak of O−H stretching vibration in the aqueous phase, the peak of O−H stretching vibration obtained at ∼3200 cm^{-1}, which corresponds to the hydrogen-

Table 1. Three-Phase Equilibrium Data (Temperature T, Pressure p) of the HFC-32 (2) + Water (1) Binary System Containing Gas Hydrates

T/K	p/MPa	T/K	p/MPa
HL_1G		HL_1G	
275.50	0.20	291.19	1.15
276.47	0.22	291.69	1.22
277.42	0.24	292.14	1.29
278.43	0.28	292.65	1.37
279.47	0.31	HL_2G	
280.40	0.34	279.90	0.998
281.43	0.38	280.90	1.03
282.45	0.42	281.88	1.06
283.44	0.46	282.87	1.08
283.80	0.49	283.85	1.12
284.27	0.52	284.81	1.15
284.68	0.55	285.87	1.19
285.22	0.58	286.79	1.22
285.77	0.62	287.78	1.25
286.25	0.65	288.78	1.29
286.80	0.69	289.74	1.33
287.32	0.73	290.76	1.37
287.81	0.77	291.75	1.40
288.26	0.82	292.68	1.44
288.63	0.86		
289.20	0.91		
289.68	0.97		
290.20	1.03		
290.73	1.09		
HL_1L_2		L_1L_2G	
293.45	3.23	293.70	1.48
293.60	4.43	294.20	1.51
293.71	5.98	295.15	1.55
293.89	7.67	296.17	1.59
294.21	10.4	297.13	1.64
		298.17	1.68
Q_2 (HL_1L_2G)		299.12	1.72
293.16	1.45	300.09	1.74

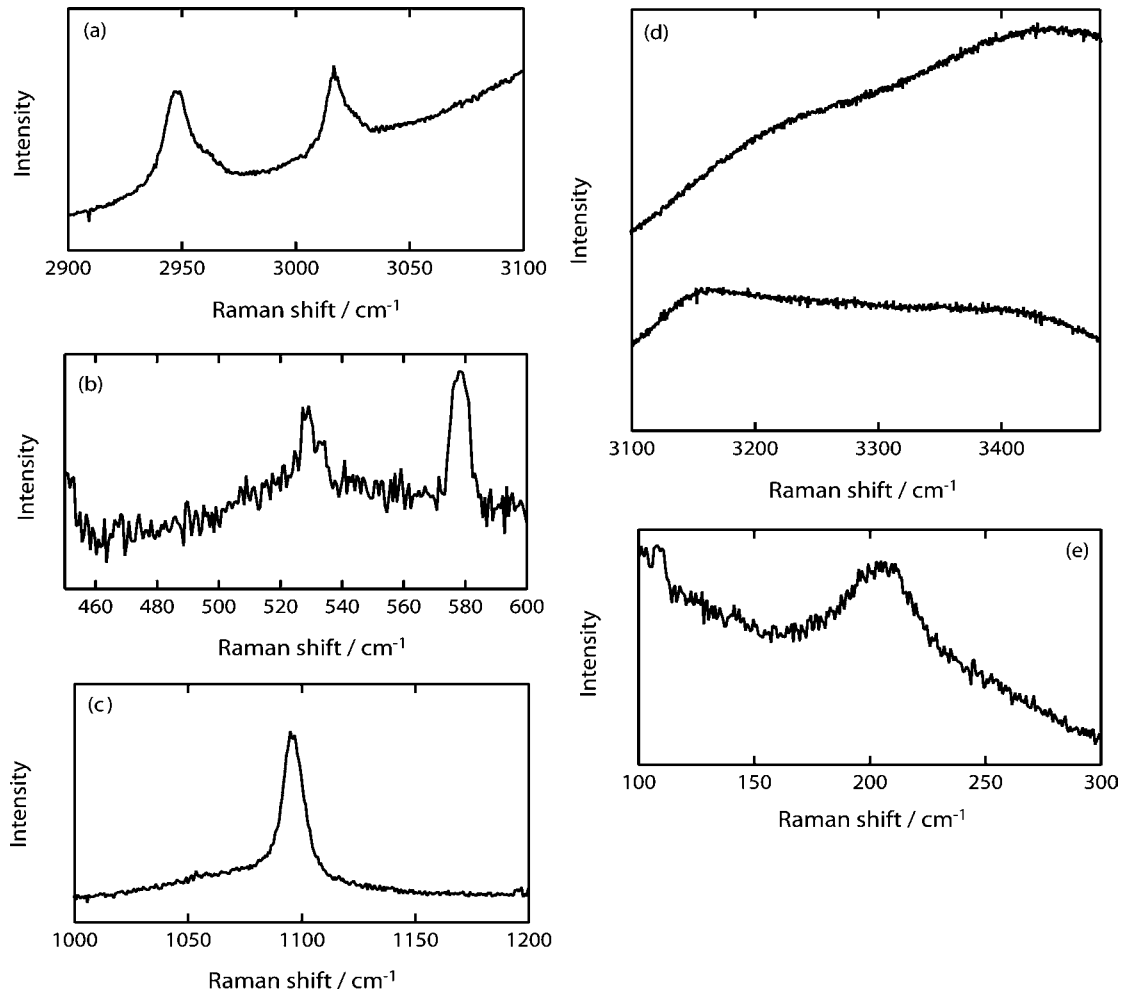

Figure 4. Raman spectra obtained in the hydrate phase for the HFC-32 + water binary system under three-phase (HL_1G) equilibrium condition of 281.80 K and 0.40 MPa. (a) Intramolecular C−H symmetric stretching vibration, (b) intramolecular F−C−F scissors vibration, (c) intramolecular C−F symmetric stretching vibration (the peak detected around 577 cm^{-1} is due to the sapphire window of high-pressure optical cell), (d) O−H stretching vibration (bottom: hydrate phase, top: aqueous phase), and (e) intermolecular O−O symmetric stretching vibration.

bonded O−H vibration mode,[16] is larger than that of ∼3400 cm^{-1} corresponding to the intramolecular O−H vibration mode. The peak shape of the O−H stretching vibration also implies that the simple HFC-32 hydrate forms the s-I hydrate.[17] In addition, the Raman shift (∼205 cm^{-1}) of the peak derived from intermolecular O−O stretching vibrations of the host water molecule supports the s-I hydrate structure of simple HFC-32 hydrate.[18] Incidentally, no Raman peak corresponding to HFC-32 molecules was obtained in the gas phase because of low-pressure conditions (0.40 MPa) in the present study. However, we have already confirmed that the Raman peaks obtained in the gaseous HFC-32 at about 1.4 MPa and room temperature are slightly blue-shifted from those of HFC-32 hydrate in each C−H and C−F vibron mode.

In the $p-T$ phase diagram, the slope of $(dp/dT)_{equil}$ can be calculated at each data point on the HL_1G curve. From the combination of $(dp/dT)_{equil}$ and the molar volume of the HFC-32 hydrate, water, and gaseous HFC-32, the overall enthalpy change of hydrate formation, ΔH_{hyd}, can be calculated with Clapeyron equation (eq 1) as follows:

$$(dp/dT)_{equil} = \Delta H_{hyd}/(\Delta v_{hyd} T) \quad (1)$$

where the total volume change Δv_{hyd} is defined by eq 2:

$$\Delta v_{hyd} = v^{G}_{HFC\text{-}32} + q \cdot v^{L}_{H_2O} - v^{H} \quad (2)$$

where v^H is calculated from the lattice constant of the s-I hydrate (1.20 nm)[19] and $v^{G}_{HFC\text{-}32}$ is obtained from the Lee−Kesler equation of state.[20] The hydration number q is assumed to be 5.75 (ideal s-I hydrate), which denotes that the HFC-32 molecule can occupy both S- and M-cages. The overall enthalpy change of hydrate formation, ΔH_{hyd}, over the entire temperature range of HL_1G regardless of the Q_2 point is summarized in Table 2. Although the ΔH_{hyd} of the HFC-32 hydrate exhibits weak temperature dependency in the HL_1G region, the value averaged from (275 to 292) K is given as 70 ± 3 $kJ \cdot mol^{-1}$. In the low-temperature range (< 280 K), the ΔH_{hyd} of the HFC-32 hydrate is similar the value of those of the simple CO_2 hydrate.

Conclusion

The four three-phase equilibrium curves of HL_1G, HL_2G, HL_1L_2, and L_1L_2G (having no hydrate phase) for the HFC-32 + water binary system were measured accurately in the temperature range from (275.15 to 300.15) K and pressure range up to 11.0 MPa. The invariant quadruple point of Q_2 (HL_1L_2G) is located at 293.16 K and 1.45 MPa. The Raman spectra obtained under the three-phase (HL_1G) equilibrium conditions reveal that the HFC-32 molecule occupies both S- and M-cages in the s-I hydrate. The overall enthalpy change of HFC-32

Table 2. Overall Enthalpy Change of Hydration ΔH_{hyd} along the HL_1G Line for the HFC-32 Hydrate

T / K	Δv_{hyd} / $cm^3 \cdot mol^{-1}$	$(dp/dT)_{equil}$ / $MPa \cdot K^{-1}$	ΔH_{hyd} / $kJ \cdot mol^{-1}$
275.50	11150	0.02	66.95
276.47	9999	0.02	67.38
277.42	9217	0.03	69.57
278.43	8066	0.03	68.68
279.47	7121	0.04	68.64
280.40	6509	0.04	70.09
281.43	5779	0.04	70.37
282.45	5220	0.05	71.78
283.44	4746	0.05	73.44
283.80	4464	0.06	72.12
284.27	4222	0.06	72.13
284.68	3986	0.06	71.52
285.22	3763	0.07	71.99
285.77	3511	0.07	71.73
286.25	3327	0.08	71.98
286.80	3136	0.08	72.45
287.32	2946	0.09	72.41
287.81	2756	0.09	71.80
288.26	2601	0.10	71.49
288.63	2440	0.10	70.09
289.20	2290	0.11	70.40
289.68	2141	0.11	69.70
290.20	2002	0.12	69.35
290.73	1878	0.13	69.30
291.19	1764	0.13	68.76
291.69	1640	0.14	67.84
292.14	1534	0.15	66.93
292.65	1429	0.16	66.26

hydrate formation is virtually constant (average value: 70 ± 3 $kJ \cdot mol^{-1}$) in the HL_1G region.

Acknowledgment

The authors are grateful to the Division of Chemical Engineering, Graduate School of Engineering Science, Osaka University for the scientific support by the Gas-Hydrate Analyzing System (GHAS). The authors give their thanks to Drs. Y. Egashira, H. Sato, and T. Sugahara (Osaka University), and Dr. T. Makino (Kobe City College of Technology) for the valuable discussions and suggestions.

Literature Cited

(1) Sloan, E. D., Jr.; Koh, C. A. *Clathrate Hydrates of Natural Gases*, 3rd ed.; Taylor & Francis: New York, 2008.

(2) Brouwer, D. H.; Brouwer, E. B.; Maclaurin, G.; Lee, M.; Parks, D.; Ripmeester, J. A. Some New Halogen-containing Hydrate-formers for Structure I and II Clathrate Hydrates. *Supramol. Chem.* **1997**, *8*, 361–367.

(3) Akiya, T.; Shimazaki, T.; Oowa, M.; Matsuno, M.; Yoshida, Y. Formation Conditions of Clathrates Between HFC Alternative Refrigerants and Water. *Int. J. Thermodyn.* **1999**, *20*, 1753–1763.

(4) Liang, D.; Guo, K.; Wang, R.; Fan, S. Hydrate Equilibrium Data of 1,1,1,2-tetrafluoroethane (HFC-134a), 1,1-dichloro-1-fluoroethane (HCFC-141b) and 1,1-difluoroethane (HFC-152a). *Fluid Phase Equilib.* **2001**, *187*−*188*, 61–70.

(5) Imai, S.; Okutani, K.; Ohmura, R.; Mori, Y. H. Phase Equilibrium for Clathrate Hydrates Formed with Difluoromethane + either Cyclopentane or Tetra-*n*-butylammonium Bromide. *J. Chem. Eng. Data* **2005**, *50*, 1783–1786.

(6) Imai, S.; Miyake, K.; Ohmura, R.; Mori, Y. H. Phase Equilibrium for Clathrate Hydrates Formed with Difluoromethane or Krypton, Each Coexisting with Fluorocyclopentane. *J. Chem. Eng. Data* **2006**, *51*, 2222–2224.

(7) Uchida, T.; Ohmura, R.; Hori, A. Critical Size for Guest Molecules to Occupy Dodecahedral Cage of Clathrate Hydrates. *J. Phys. Chem. C* **2008**, *112*, 4719–4724.

(8) Nakano, S.; Moritoki, M.; Ohgaki, K. High-pressure Phase Equilibrium and Raman Microprobe Spectroscopic Studies on the CO_2 Hydrate System. *J. Chem. Eng. Data* **1998**, *43*, 807–810.

(9) Lemmon, E. W.; Huber, M. L.; McLinden, M. O. *NIST Reference Fluid Thermodynamic and Transport Properties, REFPROP ver. 8.0*, NIST Standard Reference Database 23; NIST: Gaithersburg, MD, 2007.

(10) Duefenbacher, A.; Tülk, M. Critical Properties (p_c, T_c, and ρ_c) and Phase Equilibria of Binary Mixtures of CO_2, CHF_3, CH_2F_2, and SF_6. *Fluid Phase Equilib.* **2001**, *182*, 121–131.

(11) Suzuki, I.; Shimanouchi, T. Vibration-Rotation Spectra and Molecular Force Field of Methylene Fluoride and Methylene Fluoride-d_2. *J. Mol. Spectrosc.* **1973**, *46*, 130–145.

(12) Holzer, W.; Moser, H. Intensity in the Raman Effect. II. Absolute Intensities and Depolarization Ratios for Halogen-Substituted Methanes in the Gaseous State. *J. Mol. Spectrosc.* **1968**, *25*, 123–128.

(13) Ionov, P. I.; Kosterev, A. A.; Malinovsky, A. L.; Ryabov, E. A. Vibrational Exchange in the Manifold of High-frequency Vibrations of the CH_2F_2 Molecule. *Chem. Phys.* **1993**, *178*, 363–370.

(14) Stirling, A. Raman Intensities from Kohn-Sham Calculations. *J. Chem. Phys.* **1996**, *104*, 1254–1262.

(15) Sugahara, K.; Tanaka, Y.; Sugahara, T.; Ohgaki, K. Thermodynamic Stability and Structure of Nitrogen Hydrate Crystal. *J. Supramol. Chem.* **2003**, *2*, 365–368.

(16) Hester, K. C.; White, S. N.; Peltzer, E. T.; Brewer, P. G.; Sloan, E. D. Raman Spectroscopic Measurements of Synthetic Gas Hydrates in the Ocean. *Marine Chem.* **2006**, *98*, 304–314.

(17) Schicks, J. M.; Erzinger, J.; Ziemann, M. A. Raman Spectra of Gas Hydrates - Differences and Analogies to Ice Ih and (Gas Saturated) Water. *Spectrochim. Acta, Part A* **2005**, *61*, 2399–2403.

(18) Sugahara, K.; Sugahara, T.; Ohgaki, K. Thermodynamic and Raman Spectroscopic Studies of Xe and Kr hydrates. *J. Chem. Eng. Data* **2005**, *50*, 274–277.

(19) von Stackelberg, M. Feste Gashydrate. *Naturwiss.* **1949**, *36*, 327–333.

(20) Reid, R. C.; Prausnitz, J. M.; Poling, B. E. *The Properties of Gases & Liquids*, 4th ed.; McGraw-Hill Book Company: New York, 1986; pp 47−49.

Received for review November 20, 2009. Accepted April 28, 2010.

JE9009859